Saudi Journal of Biological Sciences (2017) 24, 45–50

King Saud University

Saudi Journal of Biological Sciences

www.ksu.edu.sa
www.sciencedirect.com

ORIGINAL ARTICLE

Green synthesis of silver nanoparticles using Andean blackberry fruit extract

Brajesh Kumar *, **Kumari Smita, Luis Cumbal, Alexis Debut**

Centro de Nanociencia y Nanotecnologia, Universidad de las Fuerzas Armadas ESPE, Av. Gral. Rumiñahui s/n, Sangolqui, P.O. BOX 171-5-231B, Ecuador

Received 19 May 2015; revised 10 August 2015; accepted 1 September 2015
Available online 6 September 2015

KEYWORDS

Silver nanoparticles;
Andean blackberry;
TEM;
XRD;
FTIR;
Antioxidant

Abstract Green synthesis of nanoparticles using various plant materials opens a new scope for the phytochemist and discourages the use of toxic chemicals. In this article, we report an eco-friendly and low-cost method for the synthesis of silver nanoparticles (AgNPs) using Andean blackberry fruit extracts as both a reducing and capping agent. The green synthesized AgNPs were characterized by various analytical instruments like UV–visible, transmission electron microscopy (TEM), dynamic light scattering (DLS), X-ray diffraction (XRD) and Fourier transform infrared (FTIR) spectroscopy. The formation of AgNPs was analyzed by UV–vis spectroscopy at λ_{max} = 435 nm. TEM analysis of AgNPs showed the formation of a crystalline, spherical shape and 12–50 nm size, whereas XRD peaks at 38.04°, 44.06°, 64.34° and 77.17° confirmed the crystalline nature of AgNPs. FTIR analysis was done to identify the functional groups responsible for the synthesis of the AgNPs. Furthermore, it was found that the AgNPs showed good antioxidant efficacy (>78%, 0.1 mM) against 1,1-diphenyl-2-picrylhydrazyl. The process of synthesis is environmentally compatible and the synthesized AgNPs could be a promising candidate for many biomedical applications.

1. Introduction

In the past decade, green synthesis of nanomaterials using various plant materials is an emerging field in Nanoscience, with emphasis to avoid the use of toxic chemicals and supports the development of ecofriendly technique. Nanomaterials (1–100 nm) of different sizes and shapes have attracted considerable attention because of their unique electronic, chemical and optical properties compared to the bulk materials (Henglein, 1989; Pileni, 1997). Recently, there has been a considerable interest in colloidal noble metal nanoparticles (MNPs) such as silver, gold and platinum in industrial applications because they exhibit different colors depending on the shape, size, and the tendency of aggregation (Lee and El-Sayed, 2006). Among noble MNPs, silver nanoparticles (AgNPs) have been given more attention due to their numerous applications in catalysis (Santos et al., 2012), biomolecular detection and diagnostic (Schultz et al., 2000), therapeutic (Eckhardt et al., 2013), micro-electronics fields (Gittins et al., 2000), sensing (Kate et al., 2011) etc.

* Corresponding author. Tel.: +593 2 3989492.
E-mail address: krmbraj@gmail.com (B. Kumar).
Peer review under responsibility of King Saud University.

Production and hosting by Elsevier

http://dx.doi.org/10.1016/j.sjbs.2015.09.006
1319-562X

Several complicated and expensive methods have been employed for the synthesis of AgNPs, such as sonochemical (Kumar et al., 2014a), microwave (Yao et al., 2010), γ-rays (Rao et al., 2010), hydrothermal (Zou et al., 2007), wet chemical (Banerjee et al., 2014), laser ablation (Abid et al., 2002) and sol–gel (Gamez et al., 2013), which involve either toxic chemicals or require high capital costs, and also generate hazardous toxic wastes. Recently, the studies are focused toward greener methods for the production of large amounts of nanoparticles in non-toxic aqueous medium. Plant materials, including leaf (Kumar et al., 2014b), bark (Mehmood et al., 2014), fruit (Kumar et al., 2015a), peel (Kumar et al., 2015b), seed (Kumar et al., 2014c), and root (Shameli et al., 2012) extracts work so well in the green synthesis of AgNPs under mild experimental conditions and replacing hazardous chemicals by polyphenols, flavonoids, proteins, saponins or sugar as reducing agents as well as capping agents.

An important example of such a plant material is the dark-red color, juicy, and flavored Andean blackberry (*Rubus glaucus* Benth.) fruit. It is consumed mainly in Ecuador, Peru and Colombia as fresh, jam, juice, frozen pulp and to a minor extent as wines (Kumar et al., 2015c). We hypothesized that flavonoids, ellagitannins and anthocyanins could be applied in the green synthesis of AgNPs. Although, green synthesis of AgNPs using different plant extracts has been already explored by our research group (Kumar et al., 2014b,c, 2015a,b). In the present study, spherical AgNPs were prepared efficiently using Andean blackberry fruit extract (ABFE) as a bioreductant and stabilizer. The synthesized AgNPs were further characterized using different analytical instruments and discussed. In addition, the antioxidant efficacy of synthesized AgNPs was also evaluated against 1,1-diphenyl-2-picrylhydrazyl (DPPH·).

2. Materials and methods

2.1. Synthesis of AgNPs

Silver nitrate, $AgNO_3$, 99.0% was purchased from Spectrum, USA and DPPH·, >99.5% was purchased from Sigma Aldrich, USA. The ABFE was prepared by the earlier method (Kumar et al., 2015c). The collected fresh blackberry fruit (5 g) was washed thoroughly and heated (62–65 °C) in 50 mL of deionized water for 60 min. After cooling, the red color extract was filtered using Whatman paper No. 1. For green synthesis, 1.0 mL of ABFE was mixed with $AgNO_3$ (10 mL, 1 mM) solution and kept at 25 °C. Green synthesis of AgNPs was confirmed by the appearance of yellowish-orange solution with lapse of time.

2.2. Radical scavenging activity

The free radical scavenging activity of the AgNPs was measured by using the DPPH·-method adapted from Kumar et al. (2014b,d) with slight modifications. An aliquot (1000–200 μL) of AgNPs or control and (1000–1800 μL) of H_2O was mixed with 2.0 mL of 20 μM (DPPH·, 0.2 N) in absolute methanol. The mixture was vortexed vigorously and allowed to stand at room temperature for 30 min in the dark. Absorbance of the mixture was measured spectrophotometrically at 517 nm, and the free radical scavenging activity was calculated using Eq. (1):

$$\text{Scavenging effect } (\%) = [1 - \{\text{absorbance of sample}/\text{absorbance of control}\}] \times 100 \quad (1)$$

The scavenging percentage of all samples was plotted. The final result was expressed as % of DPPH· free radical scavenging activity (mM).

2.3. Characterization of AgNPs

The synthesized AgNps were characterized with the help of a UV–visible single beam spectrophotometer (Thermo Spectronic, GENESYS™ 8, England). Transmission electron microscopy (TEM) and selected area electron diffraction (SAED) were recorded digitally (FEI Tecnai G2 spirit twin). The hydrodynamic size distributions and polydispersity index (PDI) of nanoparticles were analyzed by using dynamic light scattering (DLS) instrumentation (HORIBA LB -550). X-ray diffraction (XRD) studies on thin films of the nanoparticle were carried out using a PANalytical brand θ–2θ configuration (generator-detector) X-ray tube copper $\lambda = 1.54$ Å and EMPYREAN diffractometer. Fourier transform infrared (FTIR-ATR) spectra were recorded on a Perkin Elmer (Spectrum two) spectrophotometer to detect the functional groups involved in nanoparticles synthesis.

3. Results and discussion

3.1. Visual and UV–visible study

Fig. 1 shows the visual studies of the AgNPs synthesis for 48 h at room temperature. The addition of ABFE to the aqueous $AgNO_3$ solution resulted in the yellowish orange color due to the surface plasmon resonance (SPR), that strongly depends on the particle size, dielectric medium and chemical surroundings (Kumar et al., 2014b,a; Kumar et al., 2015b). The reduction of aqueous Ag^+ ions by the ABFE was easily analyzed by UV–visible spectroscopy. In the 0.5 h of synthesis, the absorption spectrum shows no peaks in the range of 380–480 nm but after 3.5 h, a new peak appears around 380–480 nm. The result shows the synthesis of AgNPs started within 3.5 h after Ag^+ ions contact with the ABFE. A broad absorption peak

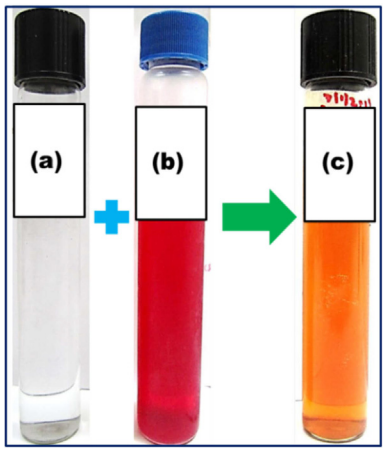

Figure 1 (a) 1 mM $AgNO_3$, (b) ABFE and (c) AgNPs.

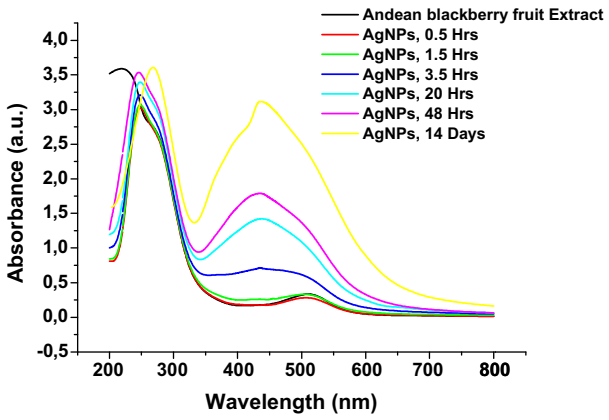

Figure 2 UV–visible absorbance spectra of as prepared AgNPs at different time intervals.

appeared at λ_{max} = 435 nm and significant absorption exists at >700 nm with lapse of time, which represents the characteristic SPR of spherical and aggregated AgNPs (Kumar et al., 2014a; Zou et al., 2007). Thus, UV–visible spectroscopy is a suitable method for initial prediction of AgNPs production (see Fig. 2).

3.2. TEM and SAED study

In Fig. 3(a–c), the resulting as-synthesized AgNPs after 48 h were predominantly of spherical shape. Higher magnification showed the average diameter of spherical AgNPs was about 12–50 nm and some are in aggregated form. Fig. 3d shows the SAED pattern recorded from the spherical AgNPs and it clearly shows the ring like electron diffraction patterns. The diffraction rings of the AgNPs have been indexed as (1 1 1), (2 0 0) and (2 2 0) consistent with the face centered cubic (fcc) structure of Ag (Tai and Yang, 2011), typical of the polycrystalline AgNPs structure (Mehmood et al., 2014).

3.3. DLS study

The average particle size distributions of AgNPs for 48 h and 14 days in DLS are 146.3 ± 76.5 nm (PDI = 0.27) and 150.7 ± 68.4 nm (PDI = 0.20) (Fig. 4). It seems to be comparable for both 48 h and 14 days, but the observed size is higher than the results of TEM images. This is due to the screening of small particles by bigger ones (Kumar et al., 2015a,b,d) as well as the presence of unreacted ABFE and also confirms the polydispersity of AgNPs (Khlebtsov and Khlebtsov, 2011). The PDI is a measure of the width of the particle size distribution and PDI less than 0.1 is typically referred to as monodisperse.

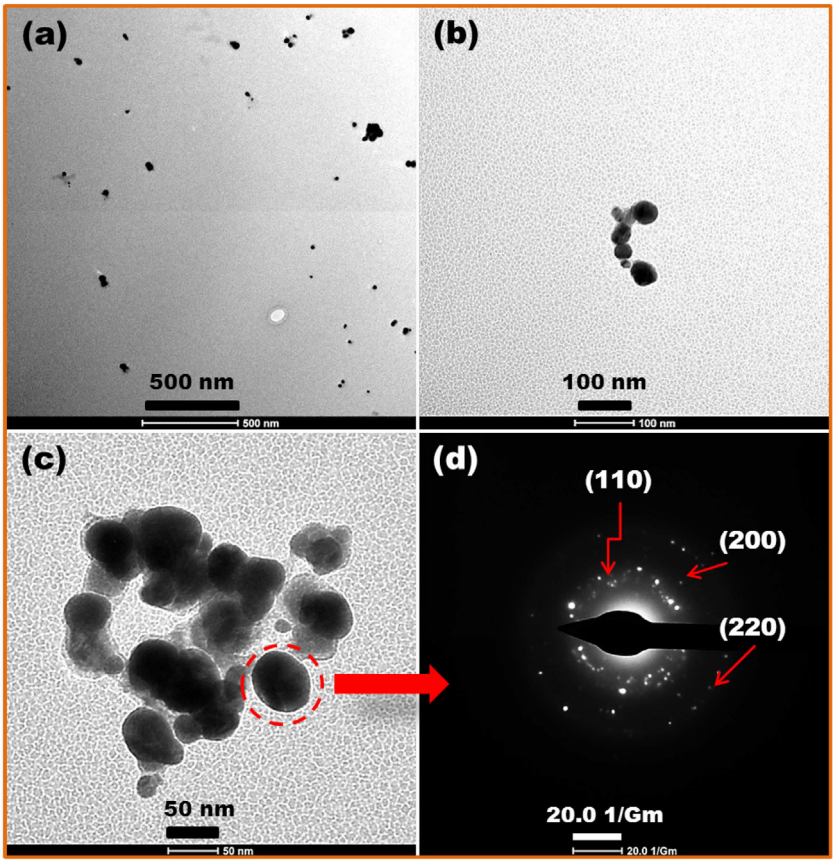

Figure 3 (a–c) TEM and (d) SAED images of AgNPs.

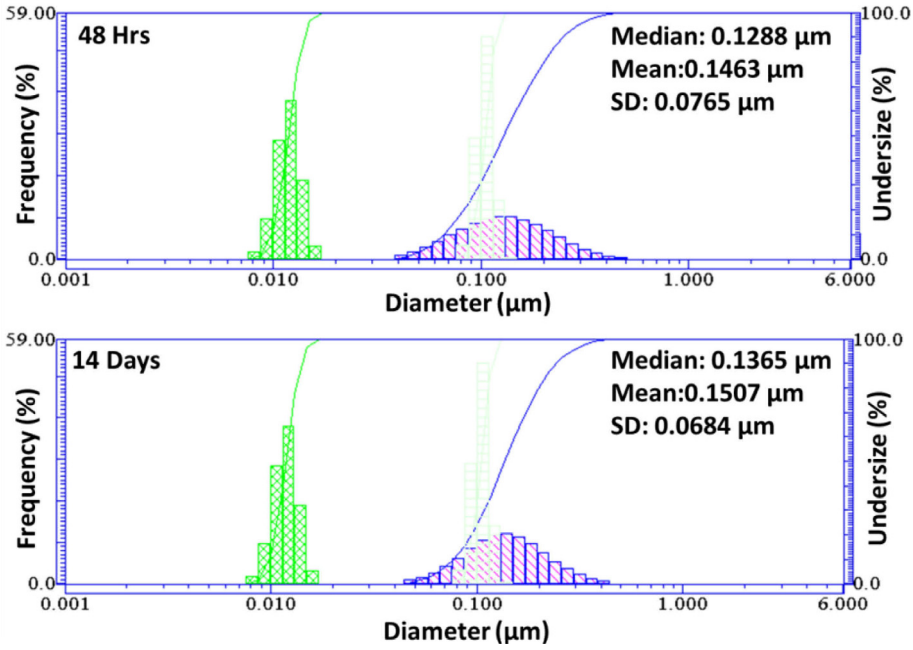

Figure 4 DLS pattern of prepared AgNPs.

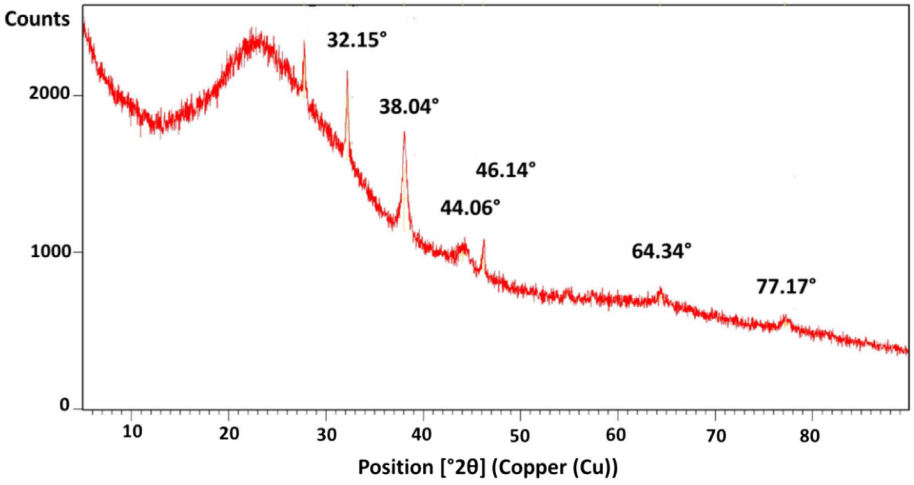

Figure 5 XRD pattern of AgNPs.

3.4. XRD study

The XRD patterns of the AgNPs synthesized by ABFE are shown in Fig. 5. The 2θ peaks observed at 38.04°, 44.06°, 64.34° and 77.17° corresponds to (111), (200), (220) and (311) reflection planes of a fcc lattice of silver (ICSD No. 98-018-0878), respectively (Kumar et al., 2015a,b). The extra peaks near to 27.7°, 32.1° and 46.1° are due to the presence of bio-organic phase on the surface of particles. Generally, the broadening of peaks in the XRD patterns of solids signifies smaller particle size and reflects the effects of the experimental conditions on the nucleation and growth of the crystal nuclei (Umadevi et al., 2012). From the XRD patterns, it indicates that the AgNP powders have large crystalline domain sizes in the mentioned concentration and correspond to pure Ag metal with fcc symmetry, consistent with those obtained from SAED pattern.

3.5. FTIR study

The FTIR spectroscopy analysis was studied to hypothesize the possible biomolecules of ABFE responsible for the synthesis of AgNPs. The peaks near 3270, 2933 and 1642 cm^{-1} (Fig. 6a) could be due to the O—H, aliphatic C—H and C═O stretching vibration of flavonoids/phenolic groups. The peak 1408 cm^{-1} corresponds for the O—H bend of

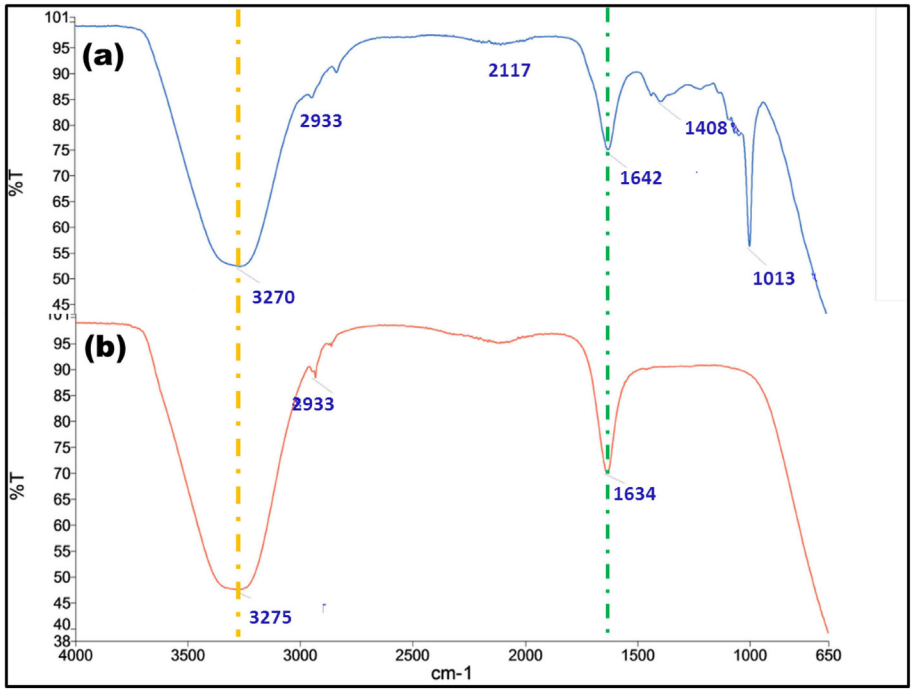

Figure 6 FTIR spectra of (a) ABFE and (b) AgNPs.

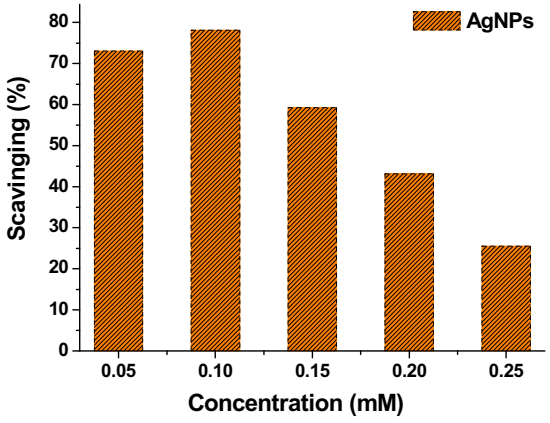

Figure 7 Antioxidative efficacy of AgNPs.

polyphenol and confirms the presence of an aromatic group, whereas the absorption peaks at 1013 cm^{-1} were assigned for C—O—C and secondary —OH group (Kumar et al., 2015c) of ABFE. In Fig. 6b, there is a deviation of peak observed for AgNPs at 3275 and 1634 cm^{-1}. It clearly suggests that the O—H and C═O groups were adsorbed on the surface of AgNPs and involved in the reduction process.

3.6. Antioxidant efficacy

The antioxidant efficacy of the AgNPs was estimated by comparing the % inhibition of DPPH· radicals (Fig. 7). It is observed that, the DPPH· radical scavenging activity of AgNPs decreases with increasing concentration (0.05 mM – 73.08%; 0.1 mM – 78.15%; 0.15 mM – 59.26%, 0.2 mM – 43.13 and 0.25 mM – 25.56%) due to the insufficient DPPH· content at higher concentration. The antioxidant effects of the AgNPs might be the result of an active physico-chemical interaction of Ag atoms with the functional groups of the ABFE (Kumar et al., 2015a,b,d).

4. Conclusions

In conclusion, the greener Andean blackberry extract for the synthesis of AgNPs is a simple, low cost and ecofriendly approach. Absorption spectra at 435 nm, confirm the presence of surface plasmon resonance of AgNPs. Analytical characterization like TEM, DLS, XRD and FTIR supports the structure, size, crystallinity and reduction mechanism of the synthesized nanoparticles. In addition, AgNPs showed efficient antioxidant efficacy (> 78%, 0.1 mM) against DPPH·, indicating it could be a promising candidate for many biomedical applications.

Acknowledgments

This scientific work has been funded by the Prometeo Project of the National Secretariat of Higher Education, Science, Technology and Innovation (SENESCYT), Ecuador.

References

Abid, J.P., Wark, A.W., Brevet, P.F., Girault, H.H., 2002. Preparation of silver nanoparticles in solution from a silver salt by laser irradiation. Chem. Commun. 2002, 792–793.

Banerjee, S., Loza, K., Meyer-Zaika, M., Prymak, O., Epple, M., 2014. Structural evolution of silver nanoparticles during wet-chemical synthesis. Chem. Mater. 26 (2), 951–957.

Eckhardt, S., Brunetto, P.S., Gagnon, J., Priebe, M., Giese, B., Fromm, K.M., 2013. Nanobio silver: its interactions with peptides and bacteria, and its uses in medicine. Chem. Rev. 113, 4708–4754.

Gamez, R.C., Castellana, E.T., Russell, D.H., 2013. Sol–gel-derived silver-nanoparticle-embedded thin film for mass spectrometry-based biosensing. Langmuir 29 (21), 6502–6507.

Gittins, D.I., Bethell, D., Nichols, R.J., Schiffrin, D.J., 2000. Diode-like electron transfer across nanostructured films containing a redox ligand. J. Mater. Chem. 10, 79–83.

Henglein, A., 1989. Small-particle research: physicochemical properties of extremely small colloidal metal and semiconductor particles. Chem. Rev. 89 (8), 1861–1873.

Kate, K.H., Damkale, S.R., Khanna, P.K., Jain, G.H., 2011. Nano-silver mediated polymerization of pyrrole: synthesis and gas sensing properties of polypyrrole (PPy)/Ag nano-composite. J. Nanosci. Nanotechnol. 11, 7863–7869.

Khlebtsov, B.N., Khlebtsov, N.G., 2011. On the measurement of gold nanoparticle sizes by the dynamic light scattering method. Colloid Journal 73 (1), 118–127.

Kumar, B., Smita, K., Cumbal, L., Debut, A., Pathak, R.N., 2014a. Sonochemical synthesis of silver nanoparticles using starch: a comparison. Bioinorg. Chem. Appl. (8 pages) 784268

Kumar, B., Smita, K., Cumbal, L., Debut, A., 2014b. Synthesis of silver nanoparticles using sacha inchi (*Plukenetia volubilis* L.) leaf extracts. Saudi J. Biol. Sci. 21, 605–609.

Kumar, B., Smita, K., Cumbal, L., Debut, A., 2014c. Sacha inchi (*Plukenetia volubilis* L.) oil for one pot synthesis of silver nanocatalyst: an ecofriendly approach. Ind. Crops Prod. 58, 238–243.

Kumar, B., Smita, K., Cumbal, L., Debut, A., 2014d. Green approach for fabrication and applications of zinc oxide nanoparticles. Bioinorg. Chem. Appl., p 7 523869.

Kumar, B., Angulo, Y., Smita, K., Cumbal, L., Debut, A., 2015a. Capuli cherry-mediated green synthesis of silver nanoparticles under white solar and blue LED light. Particuology. http://dx.doi.org/10.1016/j.partic.2015.05.005 (in press).

Kumar, B., Smita, K., Cumbal, L., Angulo, Y., 2015b. Fabrication of silver nanoplates using *Nephelium lappaceum* (Rambutan) peel: a sustainable approach. J. Mol. Liq. 211, 476–480.

Kumar, B., Smita, K., Cumbal, L., Debut, A., Angulo, Y., 2015c. Biofabrication of Copper Oxide Nanoparticles using Andean Blackberry (*Rubus glaucus* Benth.) Fruit and Leaf (in press). http://dx.doi.org/10.1016/j.jscs.2015.01.009.

Kumar, B., Smita, K., Cumbal, L., Debut, A., 2015d. *Lantana camara* berry for the synthesis of silver nanoparticles. Asian Pac. J. Trop. Biomed. 5 (3), 192–195.

Lee, K.S., El-Sayed, M.A., 2006. Gold and silver nanoparticles in sensing and imaging: sensitivity of plasmon response to size, shape, and metal composition. J. Phys. Chem. B 110, 19220–19225.

Mehmood, A., Murtaza, G., Bhatti, T.M., Raffi, M., Kausar, R., 2014. Antibacterial efficacy of silver nanoparticles synthesized by a green method using bark extract of *Melia azedarach* L. J. Pharm. Innov. 9 (3), 238–245.

Pileni, M.P., 1997. Nanosized particles made in colloidal assemblies. Langmuir 13 (13), 3266–3276.

Rao, Y.N., Banerjee, D., Datta, A., Das, S.K., Guin, R., Saha, A., 2010. Gamma irradiation route to synthesis of highly re-dispersible natural polymer capped silver nanoparticles. Radiat. Phys. Chem. 79, 1240–1246.

Santos, Kelly de O., Elias, W.C., Signori, A.M., Giacomelli, F.C., Yang, H., Domingos, J.B., 2012. Synthesis and catalytic properties of silver nanoparticle-linear polyethylene imine colloidal systems. J. Phys. Chem. C 116 (7), 4594–4604.

Schultz, S., Smith, D.R., Mock, J.J., Schultz, D.A., 2000. Single-target molecule detection with nonbleaching multicolor optical immunolabels. PNAS 97, 996–1001.

Shameli, K., Ahmad, M.B., Zamanian, A., Sangpour, P., Shabanzadeh, P., Abdollahi, Y., Zargar, M., 2012. Green biosynthesis of silver nanoparticles using Curcuma longa tuber powder. Int. J. Nanomed. 7, 5603–5610.

Tai, Y.-L., Yang, Z.-G., 2011. Fabrication of paper-based conductive patterns for flexible electronics by direct-writing. J. Mater. Chem. 21, 5938–5943.

Umadevi, M., Shalini, S., Bindhu, M.R., 2012. Synthesis of silver nanoparticle using *D. carota* extract. Adv. Nat. Sci. Nanosci. Nanotechnol. 3, 025008, 6 p.

Yao, B.H., Xu, G.C., Zhang, H.Y., Han, X., 2010. Synthesis of nanosilver with polyvinylpyrrolidone (PVP) by microwave method. Chin. J. Inorg. Chem. 26, 1629–1632.

Zou, J., Xu, T., Hou, B., Wu, D., Sun, Y., 2007. Controlled growth of silver nanoparticles in a hydrothermal process. Chin. Particuol. 5, 206–212.